

IMPROVING FACIAL ATTRIBUTE RECOGNITION BY GROUP AND GRAPH LEARNING

Zhenghao Chen[†], Shuhang Gu[†], Feng Zhu[‡], Jing Xu^{*} and Rui Zhao[‡]

[†]The University of Sydney, [‡]Sensetime Group Limited and ^{*}Applied Research Center, Tencent PCG

zhenghao.chen@sydney.edu.au, shuhangu@gmail.com, {zhufeng, zhaorui}@sensetime.com and eudoraxu@tencent.com

ABSTRACT

Exploiting the relationships between attributes is a key challenge for improving multiple facial attribute recognition. In this work, we are concerned with two types of correlations that are spatial and non-spatial relationships. For the spatial correlation, we aggregate attributes with spatial similarity into a part-based group and then introduce a Group Attention Learning to generate the group attention and the part-based group feature. On the other hand, to discover the non-spatial relationship, we model a group-based Graph Correlation Learning to explore affinities of predefined part-based groups. We utilize such affinity information to control the communication between all groups and then refine the learned group features. Overall, we propose a unified network called Multi-scale Group and Graph Network. It incorporates these two newly proposed learning strategies and produces coarse-to-fine graph-based group features for improving facial attribute recognition. Comprehensive experiments demonstrate that our approach outperforms the state-of-the-art methods.

Index Terms— Facial Attribute Recognition, Multi-Task Learning, Visual Attention, Graph Neural Network

1. INTRODUCTION

Interpreting facial attributes plays an important role in many multimedia applications (*e.g.*, face-based augmented reality). Most researchers treat facial attribute recognition as a Multi-Task Learning (MTL) problem as it normally requires to predict multiple facial attributes at once. Hence, better exploring and incorporating the correlations between different attributes can efficiently improve the recognition performance [1].

The spatial similarity is the most straightforward relationship as a certain facial region naturally corresponds to a combination of attributes [2]. A sizable body of works [1, 3, 4] have already indicated that using spatial similarity can benefit the recognition. However, existing methods simply exploited spatial similarity by extracting the shared feature from spatial-related attributes, thus had limited capacity in profiting from spatial correlation information. To better leverage the spatial correlation, we develop a method named Group Attention Learning (GAL) to apply part-based learning and spatial correlation together. We not only aggregate correlated attributes for learning shared feature extractors but also produce part-

based group attention masks. In this way, we further leverage the spatial knowledge to learn group-specific attentions, which greatly strengthens shared part-based group features.

Besides further leveraging spatial correlation to enhance intra-group feature learning, we also exploit non-spatial correlation. It refers to the fact that attributes on different facial regions may still related to each other. For instance, people having the lipstick (on the mouth) are more likely to wear the necklace (on the neck) [1]. In order to incorporate such correlation hints, some adaptive learning methods [5, 6] have been recently deployed for mining the relationships between pairs of attributes on different regions. Despite improving holistic recognition performance, the large search space [5] between pairs of attributes inevitably brings a large computation burden in the training. Moreover, all existing approaches assumed that the relationships between different attributes are undirected. Obviously, the mutual influence between attributes could be different, ignoring the direction of influence greatly affects the exploitation of correlations. To address the above issues, we develop a Graph Correlation Learning (GCL) upon our part-based groups. Concretely, a directed group-based Graph Neural Network (GNN) is conducted to explore non-spatial inter-group affinity. Such affinity is then used to update part-based group features to graph-based group features, which will contain both spatial and non-spatial information. As a result, our strategy is capable of mining directional non-spatial correlation messages between heterogeneous groups for improving recognition performance.

Overall, we propose a unified framework Multi-scale Group and Graph Network (MGG-Net) to integrate these two novel learning strategies on multi-scale feature, in which we outperform state-of-the-art approaches on prediction and balanced accuracy. Our contributions are listed as followed:

- A group attention mechanism GAL leverages intra-group spatial correlation of facial attributes and part-based learning to produce part-based group features.
- A group-based graph learning strategy GCL exploits the inter-group non-spatial correlation between part-based attribute groups to refine learned group features.
- A unified framework MGG-Net applies our approach to multi-scale feature levels and significantly improves the recognition performance on CeleBA and LFWA.

2. RELATED WORK

Facial Attribute Recognition. To estimate a single facial attribute, traditional methods mostly used hand-crafted features along with a classifier [7]. The first deep learning facial attribute prediction method was proposed by Liu *et al.* [2]. Following that, various Convolution Neural Network (CNN) methods were proposed [8, 9] to address this task. Part-based learning is the most well-known strategy for single attribute prediction. Zhang *et al.* [10] employed the facial landmarks to attain defined regions and then embedded them into Poselet. Kalayeh *et al.* [11] obtained segmentation masks from another face parsing domain and fused such masks to original features. He *et al.* [12] learned abstract facial images and leveraged them as additional part-based features. Rather than relying on auxiliary data to obtain localization cues, some recent methods attempted to use weakly-supervised approaches to generate attentions [13, 14, 15]. For example, Ding *et al.* [13] used a localization network to learn the attention for every individual attribute. In our method, we employ part-based groups to learn part-based attentions. Our design is fully based on the spatial similarity of attributes. Such affinity reduces the difficulty and complexity of attention learning. Moreover, a coarse-to-fine multi-scale architecture is employed in our network, so that different resolutions of part-based features can benefit various types of attributes.

Multi-Task Learning. MTL is a learning paradigm that jointly learns multiple tasks. Its main challenge is how to exploit relationships across different tasks so that positive correlation information can then be used to enhance holistic performance. For multiple facial attributes recognition, some MTL-based approaches aggregated attributes into groups to extract the shared feature [1, 3, 4, 16, 17]. Those works mostly designed groups according to prior spatial knowledge and only focused on the affinity inside the designed group. Differently, our method not only generates a better shared spatial feature using the group attention but also exploits the cross-group communication by a graph. Other methods used learning-based approaches to obtain the correlation. Lu *et al.* [5] adaptively learned a thin-to-wide network, while Huang *et al.* [6] employed a greedy search. Though those methods could intuitively discover non-spatial correlations, they had to explore through all attribute pairs, which causes a large search space and complexity. Differently, our method explores the graph-based non-spatial affinity through part-based groups rather than individual attributes to avoid this issue.

Graph Neural Network. GNN is proposed to deal with the non-linear data formed with graph structure. Among various GNN-based methods, our work is mostly inspired by Graph Attention Network (GAT) [18], which estimated an adjacency matrix through a multi-head attention-based mechanism. Recently, some graph-based approaches were also introduced to the pedestrian attribute prediction task [19], which learned the relationships between individual attributes. In this work, rather than building the graph upon individual

attributes, we construct a graph by taking part-based groups as nodes. In this way, we can model our exploration study to estimate inter-group non-spatial affinities from groups to groups. A two-way directed GNN is then conducted to learn bilateral relationships between part-based groups. Therefore, for each group, messages it sends to others will be distinguished from the messages it receives. Lastly, different from works [19] in pedestrian attribute estimation that used complicated multi-stage ensemble model for node processing and graph modeling, we incorporate group feature learning together with graph-based correlation learning in a unified model. So we can optimize it in an end-to-end manner.

3. METHODOLOGY

3.1. Preliminaries

Problem Formulation. Given a facial image with N pre-defined attributes a , our goal is to predict the probability Y_a for each attribute a , that achieves the minimal average prediction error $\frac{1}{N} \sum_{a=1}^N ||Y_a - \hat{Y}_a||$, where \hat{Y}_a is the attribute label.

Part-based Group. We split N facial attributes into K part-based groups according to their location similarity. We define such a group as \mathcal{G}_i , which represents the group for facial part i . $a \in \mathcal{G}_i$ indicates that attribute a is located at the part i and belongs to group \mathcal{G}_i . We then apply our approach to obtain the feature for each group \mathcal{G}_i . Such feature will be used to predict the probability Y_a for attribute a , *s.t.*, $a \in \mathcal{G}_i$.

3.2. Group and Graph Learning

We propose MGG-Net (Fig. 1 (a)) to apply our approach and produce multi-scale group features. Our backbone network extracts coarse-to-fine shared features through multi-scale feature blocks. In this work, we will use B such blocks, where \mathbf{F}_b denotes the shared feature extracted from the b th block. Our MGG-Net will then generate group features from \mathbf{F}_b by incorporating GAL (Fig. 1 (b)) and GCL (Fig. 1 (c)).

Group Attention Learning. GAL is to obtain the part-based group features for different groups by using intra-group spatial similarity and part-based learning. On each block b , we use Group Attention Modules to extract K group attention masks from shared feature \mathbf{F}_b . Each module contains a set of convolution, batch normalization and ReLU activation layers to produce a learned group attention mask \mathbf{M}_i^b for group \mathcal{G}_i . Such mask \mathbf{M}_i^b will then be multiplied with shared feature \mathbf{F}_b and the product will be used to generate part-based group feature \mathbf{f}_i^b for group \mathcal{G}_i by global average pooling (GAP). Eventually, we will obtain $B \times K$ such part-based group features \mathbf{f}_i^b , where B is the number of blocks and K is the number of groups. The process is denoted as Eq (1), where ϕ represents Group Attention Modules and θ_i^b are learned parameters.

$$\begin{aligned} \mathbf{M}_i^b &= \phi(\mathbf{F}_b, \theta_i^b) \\ \mathbf{f}_i^b &= \text{GAP}(\mathbf{F}_b \mathbf{M}_i^b) \end{aligned} \quad (1)$$

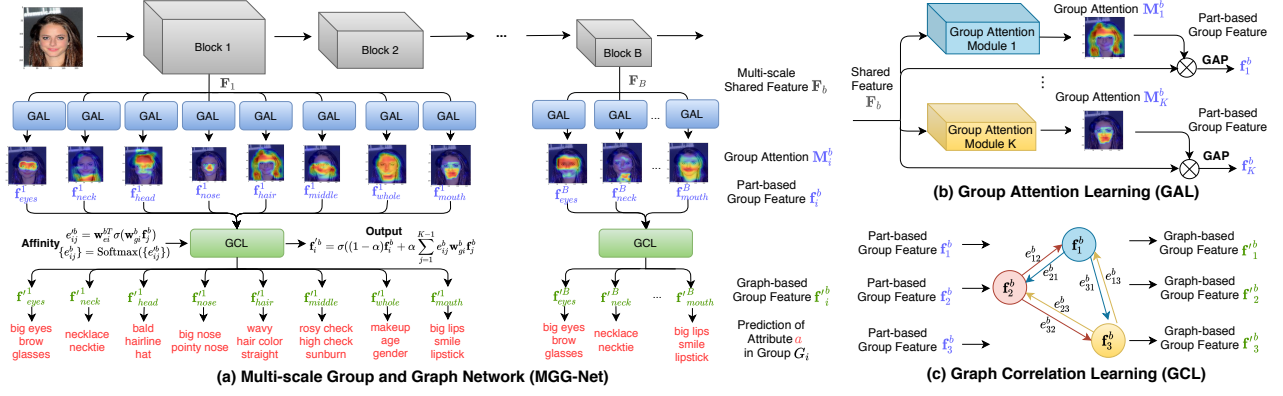


Fig. 1. An overview of our MGG-Net (a), GAL (b) and GCL (c). We assign multiple attributes a to different part-based groups \mathcal{G}_i according to their spatial similarity. The backbone first extracts multi-scale shared feature F_b from the b th block. Then, GAL will generate group attention mask M_i^b for each \mathcal{G}_i from F_b . Such mask M_i^b will multiply with F_b and produce the part-based group feature f_i^b by global average pooling (GAP). After that, GCL will update part-based group feature f_i^b to graph-based group feature $f_i^{b'}$ by using affinities between part-based groups. Eventually, $f_i^{b'}$ will contain both group-based spatial and graph-based non-spatial correlation information. It would then be used to predict all facial attributes a in part-based group \mathcal{G}_i .

Graph Correlation Learning. While GAL manipulates the spatial correlation of attributes inside a part-based group, GCL will be used to explore the non-spatial inter-group affinity between all part-based groups to enhance the group features. Specifically, we build a two-way directed GNN to model part-based group features f_i^b at scale b . Here, we use the learned part-based group features f_i^b from GAL as nodes and the affinity values sent from f_j^b to f_i^b , e_{ij}^b , as edges. We assume that the message sent from f_j^b to f_i^b is not identical to the message from f_i^b to f_j^b (i.e., $e_{ij}^b \neq e_{ji}^b$). Then, f_i^b will be updated by all affinity values of e_{ij}^b , which are received from other nodes f_j^b . To compute such values, we learn a graph transfer weight w_{gi}^b and an edge weight w_{ei}^b for the node f_i^b . The node f_j^b will be multiplied by w_{gi}^b and then activated by a ReLU activation function. After that, we multiply the transpose of w_{ei}^b to compute a value e_{ij}^b . A Softmax function will then be applied for the value set $\{e_{ij}^b\}$ to produce the affinity value set $\{e_{ij}^b\}$ with $K-1$ values. Once we obtain all affinity values e_{ij}^b , the network will update part-based group feature f_i^b to graph-based group feature $f_i^{b'}$ by the layer-wise graph attention mechanism. To this end, the graph-based group feature $f_i^{b'}$ would contain both its own part-based information and correlation information from other part-based group features. The process is denoted as Eq (2), where the σ represents ReLU activation function and α is a constant number.

$$\begin{aligned}
e_{ij}^b &= \mathbf{w}_{ei}^{bT} \sigma(\mathbf{w}_{gi}^b \mathbf{f}_j^b) \\
\{e_{ij}^b\} &= \text{Softmax}(\{e_{ij}^b\}) \\
\mathbf{f}_i^{b'} &= \sigma((1-\alpha)\mathbf{f}_i^b + \alpha \sum_{j=1}^{K-1} e_{ij}^b \mathbf{w}_{gi}^b \mathbf{f}_j^b)
\end{aligned} \tag{2}$$

3.3. Multi-Task Prediction and Optimization

Recalling that our goal is to predict the probability Y_a for each attribute a , while our GAL and GCL can generate part-based group features f_i^b and graph-based group features $f_i^{b'}$. We can predict GAL-based probabilities $Y_a^{b,GAL}$ and GCL-based probabilities $Y_a^{b,GCL}$ by using f_i^b and $f_i^{b'}$ for all attributes a , s.t., $a \in \mathcal{G}_i$. In addition, we also use the shared feature F_B extracted from the last block B to obtain a base prediction Y_a^B for the attribute a . All prediction processes are denoted as Eq (3), where γ represents the binary classifier, θ denotes learned parameters and ψ is the Sigmoid activation function.

$$\begin{aligned}
Y_a^{b,GAL} &= \psi(\gamma(\mathbf{f}_i^b, \theta_a^b)) \quad s.t. \ a \in \mathcal{G}_i \\
Y_a^{b,GCL} &= \psi(\gamma(\mathbf{f}_i^{b'}, \theta_a^b)) \quad s.t. \ a \in \mathcal{G}_i \\
Y_a^B &= \psi(\gamma(\mathbf{F}_B, \theta_a^B))
\end{aligned} \tag{3}$$

The eventual prediction Y_a is then calculated by averaging predictions $Y_a^{b,GCL}$ from graph-based group feature $f_i^{b'}$ on all blocks and base prediction Y_a^B from the last shared feature F^B . It is denoted as Eq (4), where B is the number of blocks.

$$Y_a = \frac{(Y_a^B + \sum_{b=1}^B Y_a^{b,GCL})}{1+B} \tag{4}$$

We optimize the entire network by summing all individual prediction lossless \mathcal{L} from each parts. Specifically, we take $N \times B$ losses from $Y_a^{b,GAL}$ to optimize GAL, $N \times B$ losses from $Y_a^{b,GCL}$ to optimize GCL, N losses from Y_a^B to optimize base prediction and N losses from Y_a to optimize final prediction. The total loss is denoted as Eq (5), where N is the number of attributes and \hat{Y}_a is the attribute label.

$$\mathcal{L}_{total} = \left[\sum_{a=1}^N \mathcal{L}(Y_a, \hat{Y}_a) + \sum_{a=1}^N \mathcal{L}(Y_a^B, \hat{Y}_a) + \sum_{b=1}^B \sum_{a=1}^N \mathcal{L}(Y_a^{b,GAL}, \hat{Y}_a) + \sum_{b=1}^B \sum_{a=1}^N \mathcal{L}(Y_a^{b,GCL}, \hat{Y}_a) \right] \quad (5)$$

Importantly, in this work, we aim to enhance both prediction accuracy [2] and balanced accuracy [20]. For prediction optimization, we adopt a binary cross-entropy loss for each \mathcal{L} . While for balanced optimization, we employ a weighted binary cross-entropy loss (\propto imbalance level) for each \mathcal{L} .

4. EXPERIMENT

4.1. Experiment Protocols

Datasets. We use two public facial attribute datasets CeleBA [2] and LFWA [2] for evaluation. CeleBA contains 202,599 facial images with 10K identities. It is split into 162K images for training, 20K images for validation and 20K images for testing. Each image contains 40 attribute labels. It also provides other ground truth data such as landmarks. In our experiments, we only use cropped facial images with attribute labels but not any other supervised data. LFWA is another smaller dataset with 13,233 images and 5,749 identities. It is split into two partitions: the training set with 6,263 images and the testing set with 6,970 images. Each image is annotated with 40 attributes, which are the same as CeleBA.

Evaluation Metrics. We employ two metrics: prediction accuracy and balanced accuracy. Prediction accuracy is the standard matrix used by previous works [2]. This matrix measures the overall performance but somehow ignores the class-imbalanced issue. To demonstrate that our method can also perform well for highly-skewed class distribution, we also adopt the balanced accuracy matrix as in [20]. In the next section, we will show mean results of 40 attributes for both metrics on CeleBA and prediction accuracy on LFWA.

Implementation. To apply our method, we divide 40 attributes into 8 groups based on their annotations. We adopt ResNet18 pre-trained on ImageNet as our backbone and apply GAL and GCL on the last layers of block 3 and block 4. For training our MGG-Net, we utilize 3 NVIDIA GTX 1080Ti and set the batch size as 144. The network is trained end-to-end. Specifically, for prediction accuracy on CeleBA, we train 9 epochs with learning rate 0.01 and the subsequent 5 epochs with 0.001. For balanced accuracy on CeleBA, we train 12 epochs with learning rate 0.01 and the subsequent 3 epochs with 0.001. For prediction accuracy on LFWA, we train 10 epochs with learning rate 0.01 and the subsequent 5 epochs with 0.001. The input image is scaled as $224 \times 224 \times 3$ and random flip is used as data argumentation. We also implement a baseline network by only using base prediction results Y_a^B (see details in Section 3.3) with above settings.

4.2. Experiment Results

Prediction Accuracy. Table 1 reports the mean prediction accuracy results of 40 attributes on CeleBA and LFWA. In fact, most reported methods utilized extra data besides attribute labels. For example, PANDA [10] and FaceTracer [7] adopted landmarks. Walk and Learn [21] obtained 5 million online sources. Off-the-Shell [8] used another large face recognition dataset. Kalayeh *et al.* [11] and He *et al.* [12] trained their segmentation and generation networks on a large face parsing domain. Differently, our approach does not rely on any auxiliary ground-truth data and our network is trained end-to-end.

Method	CeleBA (%)	LFWA (%)
(Kumar <i>et al.</i> 2009) FaceTracer [7]	81.12	73.93
(Zhang <i>et al.</i> 2014) PANDA [10]	85.00	81.00
(Liu <i>et al.</i> 2015) ANet+LNet [2]	87.30	84.00
(Zhong <i>et al.</i> 2016) Off-the-Shell [8]	86.60	85.90
(Wang <i>et al.</i> 2016) Walk and Learn [21]	88.00	-
(Rudd <i>et al.</i> 2016) Separate [9]	90.22	-
(Rudd <i>et al.</i> 2016) MOON [9]	90.94	-
(Hand <i>et al.</i> 2017) MCNN-AUX [1]	91.26	86.30
(Lu <i>et al.</i> 2017) SOMP joint branch-32 [5]	90.40	-
(Lu <i>et al.</i> 2017) SOMP joint branch-64 [5]	91.02	-
(Kalayeh <i>et al.</i> 2017) Avg Pooling [11]	90.86	85.27
(Kalayeh <i>et al.</i> 2017) SSG [11]	91.62	86.13
(Kalayeh <i>et al.</i> 2017) SSP [11]	91.67	86.80
(Kalayeh <i>et al.</i> 2017) SSG + SSP [11]	91.80	87.13
(Huang <i>et al.</i> 2018) GNAS (Thin) [6]	91.30	86.16
(Huang <i>et al.</i> 2018) GNAS (Wide) [6]	91.63	86.37
(He <i>et al.</i> 2018) Original [12]	91.50	84.79
(He <i>et al.</i> 2018) Abstract + Original [12]	91.81	85.28
(Zhao <i>et al.</i> 2019) CSN w/o share [22]	91.70	-
(Zhao <i>et al.</i> 2019) CSN [22]	91.80	-
Ours: Baseline	91.23	85.63
Ours: MGG-Net	92.00	87.20

Table 1. Mean prediction accuracy (in %) of 40 attributes on CeleBA and LFWA compared to state-of-the-art methods.

Our baseline and MGG-Net contain 11M and 12.8M parameters. Thanks to the group structure, it totally costs 1.8M parameters for GAL and GCL only. With 16% additional parameters, our approach reduces 9.6% and 10.92% relative classification errors on CeleBA and LFWA respectively. Compared to ours, MOON [9] had 119.73M parameters and ANet+LNet [2] costed 128M parameters. He *et al.* [12] took ResNet50 which had at least 50M parameters. SSG+SSP [11] and MCNN-Aux [1] had around 24M and 16M parameters. Though our parameters cost is slightly larger than SOMP [5] (10.53M), it is still fair to claim that MGG-Net achieves the highest results using a relatively light-weight setting.

In terms of improvement on CeleBA, most methods enhanced from baselines by 0.3% - 0.9% for mean prediction accuracy. Specifically, MOON [9] outperformed its separated method by 0.72%. SSG and SSP [11] enhanced 0.76% and 0.81% respectively from only using average pooling. Abstract method [12] also contributed a 0.31% points gain from only using original images. While our proposed MGG-Net

achieves 0.77% enhancement from our baseline network. For LFWA, it is observed that MGG-Net makes 1.57% points improvement from the baseline network and has outstanding performance against all other methods. Compared to the most recent state-of-the-art approach that used abstract images [12], we even improve 1.92%. Moreover, our MGG-Net is also significantly superior over other MTL-based approaches on both CeleBA and LFWA, which are hand-designed grouping method MCNN-Aux [1], adaptive correlation learning method SOMP [5] and greedy search method GNAS [6].

Balanced Accuracy. We also demonstrate the effectiveness of our approach in the balanced setting. We compare our approach with four recent deep imbalance learning methods LMLE [20], CRL [23], CLMLE [20] and DCL [24] on CeleBA dataset. To our best knowledge, there are no existing methods evaluated the balanced task on LFWA dataset.

Method	Balanced Accuracy (%)
(Huang <i>et al.</i> 2016) LMLE [20]	83.83
(Dong <i>et al.</i> 2017) CRL [23]	86.60
(Huang <i>et al.</i> 2018) CLMLE [20]	88.78
(Wang <i>et al.</i> 2019) DCL [24]	89.05
Ours: Baseline:	88.15
Ours: MGG-Net:	89.19

Table 2. Mean balanced accuracy (in %) of 40 attributes on CeleBA dataset compared to other state-of-the-art methods.

As shown in Table 2, our MGG-Net achieves the highest mean balanced accuracy 89.19% and enhances 1.04% from the baseline. We highlight two facts. First, these four methods all had high complexity. For instance, the most recent state-of-the-art method DCL [24] re-sampled its scheduler in every iteration during the training and took 300 epochs with batch size 512 for converging. While ours adopts a group-structure, which significantly reduces the complexity and only takes 15 epochs with batch size 144 for training. Second, all existing methods were only proposed for either the balanced or prediction accuracy (*e.g.*, DCL was only optimized for enhancing balanced accuracy but not for prediction accuracy). While our approach is able to achieve excellent results on both evaluation metrics by simply switching the training criterion.

4.3. Ablation Study

Visualization of Group Attention Masks. We visualize the group attention masks to study the effectiveness of GAL. In our implementation, we extract eight $28 \times 28 \times 1$ masks from block 3 and eight $14 \times 14 \times 1$ masks from block 4 of ResNet18.

Fig. 2 shows output masks on each block. It is observed that attentions on block 3 can better outline the finer and smaller regions which correspond to eyes, mouth, nose, and hairline. While masks on block 4 perform better on the coarser and larger regions which are the whole face, around head, neck and middle face. It indicates that coarse-to-fine multi-scale design can benefit different types of facial parts.

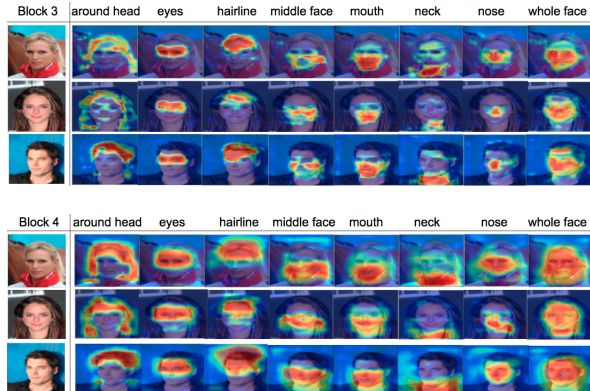


Fig. 2. Visualization of output group attention masks on block 3 ($28 \times 28 \times 1$) and block 4 ($14 \times 14 \times 1$) of ResNet18.

Effectiveness of GAL and GCL. To demonstrate the effectiveness of GAL and GCL, we further implement two networks: the first one learns all attribute attentions independently (Independent) and the second one only applies group attentions (w/o GCL). We use the same design choice and training scheme as MGG-Net (see *Implementation*) for evaluating them on LFWA. Results are shown in Table 3.

Layer	Independent (%)	w/o GCL (%)	MGG-Net (%)
Block 3	81.04	82.40	86.40
Block 4	85.27	86.42	86.81
Block 3+4	86.17	86.77	87.20

Table 3. Mean prediction accuracy (in %) on LFWA dataset by using independent attentions (Independent), only using GAL (w/o GCL), and using both GAL and GCL (MGG-Net).

It shows that GAL enhances the performance from using independent attentions by more than 1% on both block 3 and block 4. There are 40 attributes but only 8 groups, so that using independent attentions costs extra 4 times parameters than using group attentions. Hence, it indicates that GAL not only reduces parameters, but also improves performance. We also see that results on both block 3 and block 4 are enhanced by further collaborating with GCL. Moreover, GCL helps to improve overall performance (block 3 + 4 improves 0.43%).

Backbone	Baseline (%)	w/o GCL (%)	MGG-Net (%)
Resnet18	85.63	86.77	87.20
Resnet34	85.65	86.42	86.81
VGG16	84.57	84.06	85.22
AlexNet	84.30	84.90	85.59

Table 4. Mean prediction accuracy (in %) on LFWA with different backbones for our baseline, the network only using GAL (w/o GCL), and MGG-Net using both GAL and GCL.

We also show the effectiveness of our method by switching different backbones for our baseline, the network only using GAL and our MGG-Net using both GCL and GAL. The results in Table 4 indicate that our GCL and GAL consistently boost the accuracy with different backbones. While simply increasing parameters by changing backbones or only using GAL does not necessarily improve the performance.

5. CONCLUSION

In this work, we have proposed a novel method to enhance facial attribute recognition by exploiting and leveraging both spatial and non-spatial correlations between attributes. Our MGG-Net achieves new state-of-the-art results in the evaluation. Moreover, the ablation study shows that GAL is efficient to obtain good part-based group features by intra-group spatial similarity, while GCL can further enhance group features by inter-group non-spatial affinity. Overall, by better handling correlations between multiple facial attributes, our method is sufficient to improve the holistic recognition performance.

6. REFERENCES

- [1] Emily M Hand and Rama Chellappa, "Attributes for improved attributes: A multi-task network utilizing implicit and explicit relationships for facial attribute classification," in *AAAI*, 2017.
- [2] Ziwei Liu, Ping Luo, Xiaogang Wang, and Xiaoou Tang, "Deep learning face attributes in the wild," in *ICCV*, 2015.
- [3] Jiajiong Cao, Yingming Li, and Zhongfei Zhang, "Partially shared multi-task convolutional neural network with local constraint for face attribute learning," in *CVPR*, 2018.
- [4] Hu Han, Anil K Jain, Fang Wang, Shiguang Shan, and Xilin Chen, "Heterogeneous face attribute estimation: A deep multi-task learning approach," in *Transactions of Pattern Analysis and Machine Intelligence*, 2018.
- [5] Yongxi Lu, Abhishek Kumar, Shuangfei Zhai, Yu Cheng, Tara Javidi, and Rogerio Feris, "Fully-adaptive feature sharing in multi-task networks with applications in person attribute classification," in *CVPR*, 2017.
- [6] Siyu Huang, Xi Li, Zhi-Qi Cheng, Zhongfei Zhang, and Alexander Hauptmann, "Gnas: A greedy neural architecture search method for multi-attribute learning," in *ACM Multimedia*, 2018.
- [7] Neeraj Kumar, Peter Belhumeur, and Shree Nayar, "Facetracer: A search engine for large collections of images with faces," in *ECCV*, 2008.
- [8] Yang Zhong, Josephine Sullivan, and Haibo Li, "Face attribute prediction using off-the-shelf cnn features," in *ICB*, 2016.
- [9] Ethan M Rudd, Manuel Günther, and Terrance E Boulton, "Moon: A mixed objective optimization network for the recognition of facial attributes," in *ECCV*, 2016.
- [10] Ning Zhang, Manohar Paluri, Marc'Aurelio Ranzato, Trevor Darrell, and Lubomir Bourdev, "Panda: Pose aligned networks for deep attribute modeling," in *CVPR*, 2014.
- [11] Mahdi M Kalayeh, Boqing Gong, and Mubarak Shah, "Improving facial attribute prediction using semantic segmentation," in *CVPR*, 2017.
- [12] Keke He, Yanwei Fu, Wuhao Zhang, Chengjie Wang, Yu-Gang Jiang, Feiyue Huang, and Xiangyang Xue, "Harnessing synthesized abstraction images to improve facial attribute recognition," in *IJCAI*, 2018.
- [13] Hui Ding, Hao Zhou, Shaohua Kevin Zhou, and Rama Chellappa, "A deep cascade network for unaligned face attribute classification," in *AAAI*, 2018.
- [14] Jianshu Li, Fang Zhao, Jiashi Feng, Sujoy Roy, Shuicheng Yan, and Terence Sim, "Landmark free face attribute prediction," in *Transactions on Image Processing*, 2018.
- [15] Wen Ji, Kelei He, Jing Huo, Zheng Gu, and Yang Gao, "Unsupervised domain attention adaptation network for caricature attribute recognition," in *ECCV*, 2020.
- [16] Sixue Gong, Xiaoming Liu, and Anil K Jain, "Jointly de-biasing face recognition and demographic attribute estimation," in *ECCV*, 2020.
- [17] Jie Yang, Jiarou Fan, Yiru Wang, Yige Wang, Weihao Gan, Lin Liu, and Wei Wu, "Hierarchical feature embedding for attribute recognition," in *CVPR*, 2020.
- [18] Petar Velickovic, Guillem Cucurull, Arantxa Casanova, Adriana Romero, Pietro Lio, and Yoshua Bengio, "Graph attention networks," in *ICLR*, 2018.
- [19] Qiaozhe Li, Xin Zhao, Ran He, and Kaiqi Huang, "Visual-semantic graph reasoning for pedestrian attribute recognition," in *AAAI*, 2019.
- [20] Chen Huang, Yining Li, Change Loy Chen, and Xiaoou Tang, "Deep imbalanced learning for face recognition and attribute prediction," in *Transactions on Pattern Analysis and Machine Intelligence*, 2019.
- [21] Jing Wang, Yu Cheng, and Rogerio Schmidt Feris, "Walk and learn: Facial attribute representation learning from egocentric video and contextual data," in *CVPR*, 2016.
- [22] Xiangyun Zhao, Yi Yang, Feng Zhou, Xiao Tan, Yuchen Yuan, Yingze Bao, and Ying Wu, "Recognizing part attributes with insufficient data," in *ICCV*, 2019.
- [23] Qi Dong, Shaogang Gong, and Xiatian Zhu, "Imbalanced deep learning by minority class incremental rectification," in *Transactions on Pattern Analysis and Machine Intelligence*, 2018.
- [24] Yiru Wang, Weihao Gan, Jie Yang, Wei Wu, and Junjie Yan, "Dynamic curriculum learning for imbalanced data classification," in *ICCV*, 2019.